# Controlled Synthesis of CdTe and CdSe Multiblock Heteronanostructures

Lifei Xi,[†] Chris Boothroyd,[‡,§] and Yeng Ming Lam*,[†]

*Department of Materials Science and Engineering, Nanyang Technological University, Singapore 639798, Institute of Materials Research and Engineering, 3 Research Link, Singapore 117602, Singapore, and Center for Electron Nanoscopy, Technical University of Denmark, DK-2800 Kongens, Lyngby, Denmark*

*Received August 31, 2008. Revised Manuscript Received January 6, 2009*

We have successfully synthesized a novel cadmium telluride and cadmium selenide multiple-block heteronanostructure using the hot coordinating solvents method. Using this method, we grew CdSe at each end of the CdTe nanorods and then grew CdTe at the ends of the CdSe/CdTe/CdSe rods. This heterogeneous nanorod architecture is different from previous studies where a linear CdSe block is first synthesized and then CdTe extensions are grown on the ends of the CdSe. High resolution transmission electron microscopy (HRTEM) of the heterostructure shows that the CdSe and CdTe rich parts of the nanorods both have the wurtzite crystal structure and that stacking faults are common. In this report, EELS line scans accompanied by optical analysis (ultraviolet−visible and photoluminescence) and thin film X-ray diffraction of the prepared nanoparticles were used to confirm the formation of heteronanostructures.

## Introduction

Heteronanostructure (HNS) dots or rods represent a convenient approach to the development of nanoscale building blocks, because they combine inorganic parts with different functionalities in the same particle.[1,2] Such a structure can restrict the movement of charge carriers (electrons or holes) and forces them into quantum confinement leading to a set of discrete energy levels at which the carriers can exist.[3] It is found by Peng et al. that HNSs have rise times and biexponential decays longer than those of nanorods with similar dimensions. In photovoltaic applications longer charge carrier or recombination lifetimes are desirable because more charge can be transferred.[4] Furthermore, the proximity between the different blocks may be an advantage from the charge separation point of view. Blocks based on semiconductor nanorods will exhibit a lower lasing threshold, emit linearly polarized light, and also give rise to improved power conversion efficiency for photovoltaic applications.[5−8] The formation of these structures is essential for future applications of semiconductor nanoparticles in nanoscale devices and important in the exploitation of the properties of nanomaterials. However, the strategies currently employed to connect quantum dots or rods mainly involve the use of an organic coupling agent.[9,10] These methods have limited control over the coupling conditions and the geometry and complexity of the assemblies.[11]

As an alternative to the organic coupling method, a great deal of research has been done on direct synthesis of heterostructure nanorods or nanowires using vapor−liquid−solid (VLS),[12] solution−liquid−solid (SLS),[13] or chemical vapor deposition (CVD).[14] Dick et al. synthesized multiple branched GaP nanotrees via the VLS growth mode with the aid of gold aerosol nanoparticle catalyst activation.[12] Wu et al. developed a hybrid pulsed laser ablation−CVD (PLA-CVD) process for the synthesis of block-by-block Si/SiGe heteronanowires.[14] However, there are some disadvantages related to these methods. One disadvantage is that there is little control over the dimensions of the heteronanowires; their diameters can vary by several hundred nanometers, and they often have a polycrystalline structure with less ideal interfaces.[14] On top of that, these methods require expensive high vacuum equipment and/or catalysts.

Alternatively, the growth of colloidal elongated nanoparticles from homogeneous solutions seems reasonable as a result of its controllable growth and simplicity. These

* Corresponding author. E-mail: ymlam@ntu.edu.sg. Fax: +65 6790 9081.
[†] Nanyang Technological University.
[‡] Institute of Materials Research and Engineering.
[§] Center for Electron Nanoscopy, Technical University of Denmark.

(1) Manna, L.; Milliron, D. J.; Meisel, A.; Scher, E. C.; Alivisatos, A. P. *Nat. Mater.* **2003**, *2*, 382.
(2) Kudera, S.; Carbone, L.; Casula, M. F.; Cingolani, R.; Falqui, A.; Snoeck, E.; Parak, J. P.; Manna, L. *Nano Lett.* **2005**, *5*, 445.
(3) Peng, P.; Milliron, D. J.; Hughes, S. M.; Johnson, J. C.; Alivisatos, A. P.; Saykally, R. J. *Nano Lett.* **2005**, *5*, 1809.
(4) Lou, Y.; Chen, X.; Samia, A. C.; Burda, C. J. *J. Phys. Chem. B* **2003**, *107*, 12431.
(5) Hu, J. T.; Li, L. S.; Yang, W. D.; Manna, L.; Wang, L. W.; Alivisatos, A. P. *Science* **2001**, *292*, 2060.
(6) Kazes, M.; Lewis, D. Y.; Ebenstein, Y.; Mokari, T.; Banin, U. *Adv. Mater.* **2002**, *14*, 317.
(7) Huynh, W. U.; Dittmer, J. J.; Alivisatos, A. P. *Science* **2002**, *295*, 2425.
(8) Jayadevan, K. P.; Tseng, T. Y. *J. Nanosci. Nanotechnol.* **2005**, *5*, 1768.
(9) Collier, C. P.; Vossmeyer, T.; Heath, J. R. *Annu. Rev. Phys. Chem.* **1998**, *49*, 371.
(10) Ouyang, M.; Awschalom, D. D. *Science* **2003**, *301*, 1074.
(11) Milliron, D. J.; Hughes, S. M.; Cui, Y.; Manna, L.; Li, J. B.; Wang, L. W.; Alivisatos, A. P. *Nature* **2004**, *430*, 190.
(12) Dick, K. A.; Deppert, K.; Larsson, M. W.; Martensson, T.; Seifert, W.; Wallenberg, R.; Samuelson, L. *Nat. Mater.* **2004**, *3*, 380.
(13) Dong, A.; Wang, F.; Daulton, T. L.; Buhro, W. E. *Nano Lett.* **2007**, *7*, 1308.
(14) Wu, Y. Y.; Fan, R.; Yang, P. D. *Nano Lett.* **2002**, *2*, 83.

10.1021/cm802350p CCC: $40.75 
Published on Web 03/23/2009

methods include the micelle or reverse micelle method,[15,16] the hydrothermal method,[17,18] and the hot coordinating solvents method.[1,3,5,11,19] These methods, especially the hot coordinating solvents method, have the potential to synthesize relatively complicated heterostructures. Several groups have actively investigated heterostructures including core/shell, linear, and three-dimensional (3D) heterostructures.[20−27] For example, Milliron et al. synthesized several cadmium chalcogenide heterostructure nanoparticles with linear and branched topologies using this method.[11] Very recently, the Korgel group synthesized CdTe/CdSe/CdTe heterostructure nanorods by sequential reactant injection.[28] They further studied the coalescence and interface diffusion of prepared heterostructure nanorods.[29]

Although several groups have reported the synthesis of a heterostructure made up of a linear CdSe block with CdTe extensions,[11,25,26,28−30] the growth of a linear CdTe block with CdSe extensions has rarely been reported. Moreover, the possibility of forming increasingly complex structures, such as multiblock HNSs, opens the door to more complex one-dimensional materials and devices exploiting the unique properties of nanomaterials. In this work, we aimed to synthesize a multiblock CdTe and CdSe HNS using the hot coordinating solvents method by sequential injection of two different precursors—TOPTe and TOPSe. This is the first attempt to synthesize multiple block HNSs with this configuration. This investigation may help in the building up of more complex functional nanoscale devices and nanomaterials because the multistep procedure allows a level of control and flexibility.

## Experimental Section

**Materials.** TOPO (trioctylphosphine oxide, 99%,) was purchased from Sigma-Aldrich. TOP (trioctylphosphine, 90%) and cadmium oxide (CdO, 99.95%) were purchased from Fluka. ODPA (octadecylphosphonic acid, 100%) and selenium (99%) were purchased from Alfa Aesar and Kanto chemical Co. Inc., respectively. Lauroyl peroxide (97%) was purchased from Lancaster. All syntheses were carried out in standard air-free conditions.

Two stock precursor solutions were prepared. For the first stock solution (TOPTe), 127.6 mg of Te powder was dissolved into 2.0 mL of TOP by heating to 80 °C. For the second stock solution (TOPSe), 78.6 mg of Se powder was dissolved into 1.5 mL of TOP at room temperature.

**Synthesis of CdSe and CdTe Multiblock HNSs.** The HNSs were prepared using a modification of Peng's procedure for cadmium chalcogen nanoparticles.[31] First, CdTe nanorods were grown in a mixture of 1.98 g of Cd-ODPA complexes (0.2054 g of CdO, 0.8928 g of ODPA, and 0.88 g of TOPO) and 2.02 g of TOPO aged overnight at 350 °C. After the temperature was stabilized at 330 °C, half of the first stock solution (TOPTe) was injected in two injections. We call this the first injection. After 4 min of reaction, 0.8 mL of the second stock solution (TOPSe) was gradually injected into the above solution using another two injections, and we called this the second injection. The reaction was carried on for an additional 5 min. The other half of the first stock solution (TOPTe) was injected into the above solution using two injections, and we called this the third injection. The reaction was stopped after 7 min. The nanoparticles were purified by precipitating the particles from toluene with excess ethanol. The nanoparticles for electron energy-loss spectroscopy (EELS) studies were etched with lauroyl peroxide to remove the ligands and to some certain extent the surface of the nanoparticles.[32]

## Characterization

Transmission electron microscopy (TEM) was carried out using a monochromated FEI Titan electron microscope with a field emission gun using acceleration voltages of 120 kV and 300 kV. TEM samples were prepared by dropping one or two drops of the HNSs solution onto carbon-coated copper grids. Electron energy-loss spectroscopy (EELS) and high angle annular dark field (HAADF) were used to study the chemical composition along the length of the HNSs. Ultraviolet−visible (UV−vis) absorption and photoluminescence (PL) spectra of the nanoparticles were obtained using a Shimadzu UV2501PC spectrophotometer and a Shimadzu RF-5301 PC fluorometer, respectively. The excitation wavelength for PL was 450 nm. All the optical measurements were performed at room temperature under ambient conditions. Thin film X-ray diffraction (XRD) studies were carried out in a Rigaku DMAX 2200 with Cu Kα radiation.

## Results and Discussion

Thin film XRD patterns from CdTe nanorods and the CdTe/CdSe multiblock HNSs are shown in Figure 1. The pattern of the CdTe nanorods indicates the presence of the hexagonal structure. In addition, the strong and sharp diffraction peak at $2\theta = 23.7°$ suggests that the crystals are extended along the *c*-axis. By comparing the diffraction pattern of the CdTe nanorods prepared after the first injection with that of bulk hexagonal CdTe, it was found that the pattern of the CdTe nanorods shows a high degree of distortion in the intensity ratios due to shape anisotropy which leads to an enhancement of the reflections associated with crystalline domains along

(15) Maillard, M.; Giorgio, S.; Pileni, M. P. *Adv. Mater.* **2002**, *14*, 1084.
(16) Xi, L. F.; Lam, Y. M. *J. Colloid Interface Sci.* **2007**, *316*, 771.
(17) Peng, Q.; Dong, Y. J.; Deng, Z. X.; Li, Y. D. *Inorg. Chem.* **2002**, *41*, 5249.
(18) Xi, L. F.; Lam, Y. M.; Xu, Y. P.; Li, L. J. *J. Colloid Interface Sci.* **2008**, *320*, 491.
(19) Xi, L. F.; Tan, W. X. W.; Boothroyd, C.; Lam, Y. M. *Chem. Mater.* **2008**, *20*, 5444.
(20) Müller, J.; Lupton, J. M.; Rogach, A. L.; Feldmann, J. *Phys. Rev. B* **2005**, *72*, 1.
(21) Hines, M. A.; Guyot-Sionnest, P. *J. Phys. Chem.* **1996**, *100*, 468.
(22) Mokari, T.; Banin, U. *Chem. Mater.* **2003**, *15*, 3955.
(23) Manna, L.; Scher, E. C.; Li, L. S.; Alivisatos, A. P. *J. Am. Chem. Soc.* **2002**, *124*, 7136.
(24) Mokari, T.; Rothenberg, E.; Popov, I.; Costi, R.; Banin, R. *Science* **2004**, *304*, 1787.
(25) Halpert, J. E.; Porter, V. J.; Zimmer, J. P.; Bawendi, M. G. *J. Am. Chem. Soc.* **2006**, *128*, 12590.
(26) Kumar, S.; Jones, M.; Lo, S. S.; Scholes, G. D. *Small* **2007**, *3*, 1633.
(27) Talapin, D. V.; Shevchenko, E. V.; Murray, C. B.; Kornowski, A.; Foerster, F.; Weller, H. *J. Am. Chem. Soc.* **2004**, *126*, 12984.
(28) Saunders, A. E.; Koo, B.; Wang, X.; Shih, C. K.; Korgel, B. A. *ChemPhysChem* **2008**, *9*, 1158.
(29) Koo, B.; Korgel, B. A. *Nano Lett.* **2008**, *8*, 2490.
(30) Jones, M.; Kumar, S.; Lo, S. S.; Scholes, G. D. *J. Phys. Chem. C* **2008**, *112*, 5423.
(31) Peng, A. Z.; Peng, X. G. *J. Am. Chem. Soc.* **2002**, *124*, 3343.
(32) Blackman, B.; Battaglia, D. M.; Mishima, T. D.; Johnson, M. B.; Peng, X. *Chem. Mater.* **2007**, *19*, 3815.

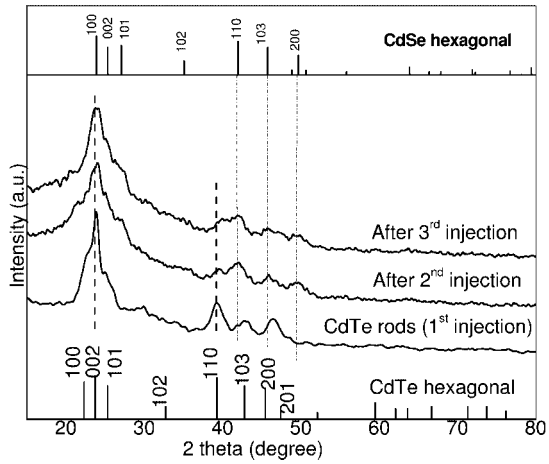


**Figure 1.** Thin film XRD patterns of CdTe nanorods and CdTe/CdSe multiblock HNSs after the second and third injection are compared with the JCPDS hexagonal CdTe and CdSe patterns.

the *c*-axis.[33] The diffraction patterns for CdTe/CdSe HNSs after the second injection show that the HNSs have the same structure as CdTe and CdSe but with slightly different lattice parameters. For example, three new peaks corresponding to hexagonal CdSe (110), (103), and (200) are present. The original peaks attributed to (002) and (110) from the CdTe nanorods can still be observed as shown in Figure 1. This suggests that CdSe is growing on CdTe epitaxially rather than as separate crystals, which is in good agreement with the HRTEM and EELS line scan analysis shown later. The (002) peak becomes broadened and shifted slightly due to the smaller lattice parameter of CdSe. After the third Te precursor injection, the peaks corresponding to (110), (103), and (200) become less sharp and the (002) peak becomes even broader. The slight shift of the (002) X-ray peak and the shift in the optical absorption (which will be discussed later) of the HNSs after the second and third injection tell us that there are at most a few monolayers of CdSe on the sides of the previously formed HNSs.[11,34] Therefore, we conclude that hexagonal CdSe and CdTe blocks grow mainly on the ends of the previously formed CdTe blocks after the secondary injection.

Representative TEM images showing evolution in size and shape of CdTe/CdSe HNS are shown in Figure 2. A comparison between the TEM images of samples taken before and after the second injection (Figure 2a,b) indicates that the mean length of the nanorods increases without any significant change in diameter upon growth of the secondary material. Different facets of a crystal have different atomic arrangements which affect the ability of a surfactant to coordinate. This results in different surface energies and therefore a variation in the growth rates on different facets. Cadmium chalcogenide nanoparticles can grow anisotropically as rods or into more complex shapes, such as branched structures in the presence of a high monomer concentration.[31,33,35,36]

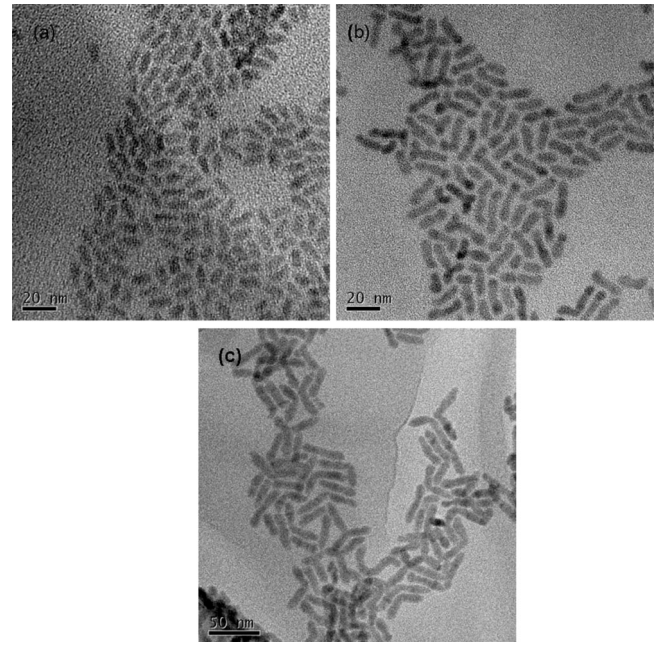


**Figure 2.** TEM images of CdTe/CdSe multiblock HNSs synthesized from (a) CdTe nanorods, (b) after the second injection and (c) after the third injection.

When these wurtzite structure materials grow in the presence of suitable surfactants, the lateral nonpolar facets have much lower growth rates than the basal polar facets, and therefore the nanoparticles grow preferentially along their unique *c*-axis.[2] The higher reactivity of the ends of such nanorods provides a higher possibility to nucleate a second material on these locations.[11,24] In Figure 2b, there are CdSe branches or irregularities growing at the ends of some of the CdTe nanorods. It is thought that the topology of each block is determined by the initial growth phase of the nucleating material.[31] The main reason for the branching after the second injection is the presence of stacking faults,[33] although the high monomer concentration may be another reason.[37−39]

It is shown in Figure 2c that the length of the HNS rods formed initially increases while the diameter increases only very slightly after the third injection. The previously formed tip or branch is the main location for further growth. It is shown that the newly added precursor (Te) prefers to grow on one tip of the previously formed HNSs. Ab initio pseudopotential calculations based on small CdSe wurtzite nanocrystals suggested that the difference in the reactivity of the various facets is due to differences in the passivating strength of the surfactant molecules.[2,40] This difference exists even between the two polar facets perpendicular to the *c*-axis. In our case, the high reactivity of the ends of the CdTe/CdSe HNS is still maintained because the length of HNSs gradually increase with the new injections. The diameter increased very slightly perhaps because of either Ostwald ripening as the precursors in the solution gradually become

(33) Peng, X. G.; Manna, L.; Yang, W. D.; Wickham, J.; Scher, E.; Kadavanich, A.; Alivisatos, A. P. *Nature* **2000**, *404*, 59.
(34) Zhong, H.; Zhou, Y.; Yang, Y.; Yang, C.; Li, Y. *J. Phys. Chem. C* **2007**, *111*, 6538.
(35) Peng, A. Z.; Peng, X. G. *J. Am. Chem. Soc.* **2001**, *123*, 1389.
(36) Manna, L.; Scher, E. C.; Alivisatos, A. P. *J. Am. Chem. Soc.* **2000**, *122*, 12700.
(37) Zhang, J. Y.; Yu, W. W. *Appl. Phys. Lett.* **2006**, *89*, 123108.
(38) Jimenez-Sandoval, S.; Melendez-Lira, M.; Hernandez-Calderon, I. *J. Appl. Phys.* **1992**, *72*, 4197.
(39) Mews, A.; Kadavanich, A.; Banin, U.; Alivisatos, A. P. *Phys. Rev. B* **1996**, *53*, R13242.
(40) Puzder, A.; Williamson, A. J.; Zaitseva, N.; Galli, G.; Manna, L.; Alivisatos, A. P. *Nano Lett.* **2004**, *4*, 2361.

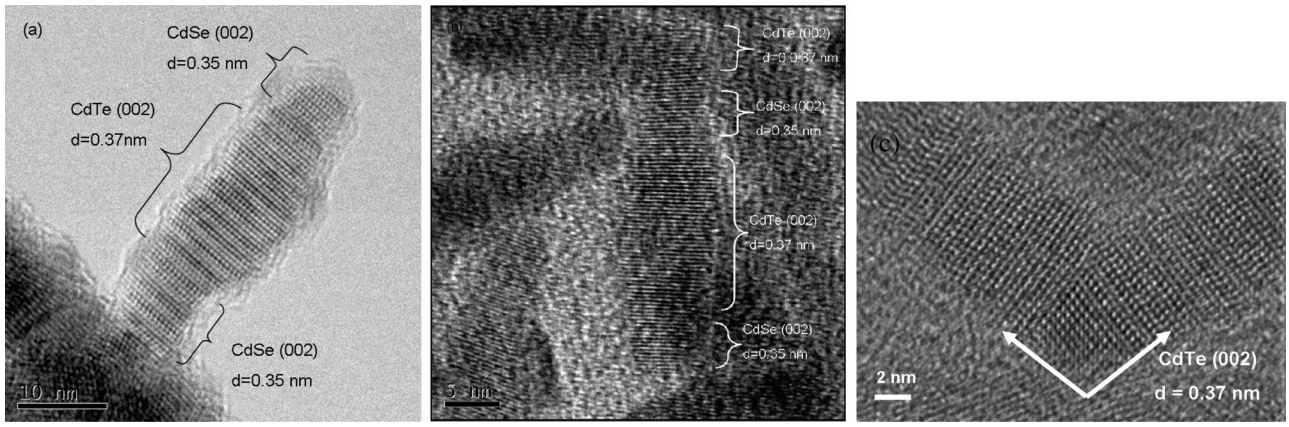


**Figure 3.** High resolution TEM images of single CdTe/CdSe HNS: (a) triblock, (b) multiblock linear extension, and (c) branch point.

depleted or the formation of a core−shell heterostructure due to overgrowth or ion exchange.[11,29]

To study the crystal structure, HRTEM was used to characterize the synthesized rods and branched HNSs as shown in Figure 3. From Figure 3a,b, it can be seen that the rods consist of a single crystal but contain stacking faults. The branched particles have original wurtzite CdTe rods as shown in Figure 3c. The structure of the interface area between the CdTe and CdSe is still unclear at this moment. A previous study by Milliron et al. showed that a zinc blende core and wurtzite branches of CdTe grew on the original wurtzite CdSe rods.[11] In this work, it is found that stacking faults are commonly found at the interfaces between the two materials. A probable reason for the presence of stacking faults at the interface is the large mismatch between the CdTe and the CdSe lattices.[37]

To confirm chemically that the rods synthesized do have CdSe and CdTe blocks, both HAADF imaging and EELS line scans were carried out. EELS is different from the energy dispersive X-ray spectroscopy (EDX) reported by other groups.[11,12,25,28,29] EELS is not affected by stray scattering and secondary fluorescence that are a problem with EDX, so EELS has a higher spatial resolution (less than 1 nm). In a HAADF image the brightness is a function of the atomic weight of the elements present and the sample thickness. If the sample has uniform thickness, any difference in brightness along the length of a single particle should correspond to differences in elemental composition. From Figure 4 it can be seen that there is a variation of the intensity along the length of the rods. But because of the variation in the thickness of the rods, it is not possible to conclusively say that there is a composition change along the HNSs.

To determine whether the rods are indeed made up of separate CdTe and CdSe blocks, we collected EELS line scans along the length of a number of HNSs. For EELS line scans a small probe is scanned along the rod and an energy loss spectrum is taken at a number of points along the length of the rod. From each energy loss spectrum the amount of Cd, Te, and Se can be determined from the areas under the respective edges. An EELS line scan from one of the rods is shown in Figure 5. We see from Figure 5b that the rod is Te rich at the center, while toward the end of the rod, especially at the left end, the rod is Se rich. Because the rods are very thin the EELS edge areas are quite noisy with

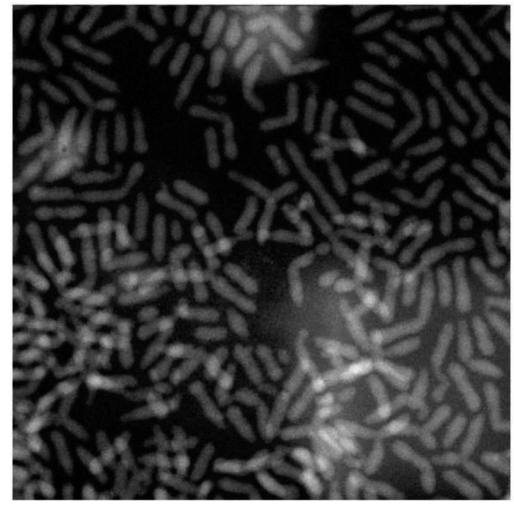

**Figure 4.** High angle annular dark-field image of HNSs.

the noise level increasing toward the ends of the rods where the thickness is lowest, hence the variability of the measured Se and Te concentrations along the length of the rods. Of the rods we analyzed, most were CdTe with a high Se concentration at one end, and a few (such as the one shown in Figure 5b) showed high Se concentrations at both ends.

The Te rich composition at the center of the rods corresponds to the first injection of the Te precursor. As we move away from the center of the rod the Se concentration increases, corresponding to the second injection of the Se precursor. As we move toward the end of the rods, the Te concentration should increase again although we did not see any evidence for this. It is likely that the etching process may have removed some material from the ends of the rods. A diagram of the growth of the HNS after each precursor injection is shown in Figure 5c.

HNSs represent unique systems because of the ability to tune the optical and electronic properties by varying the chemical composition of their components and the length of each block.[2] The absorption and PL spectra of HNSs after the second injection are shown in Figure 6. The UV−vis absorption and photoluminescence of CdTe nanorods immediately after the first injection is easily observed (see Figure 6a). The appearance of higher order features in the absorbance spectra and the sharp exciton peak indicate that the CdTe nanorods are nearly monodisperse in size and

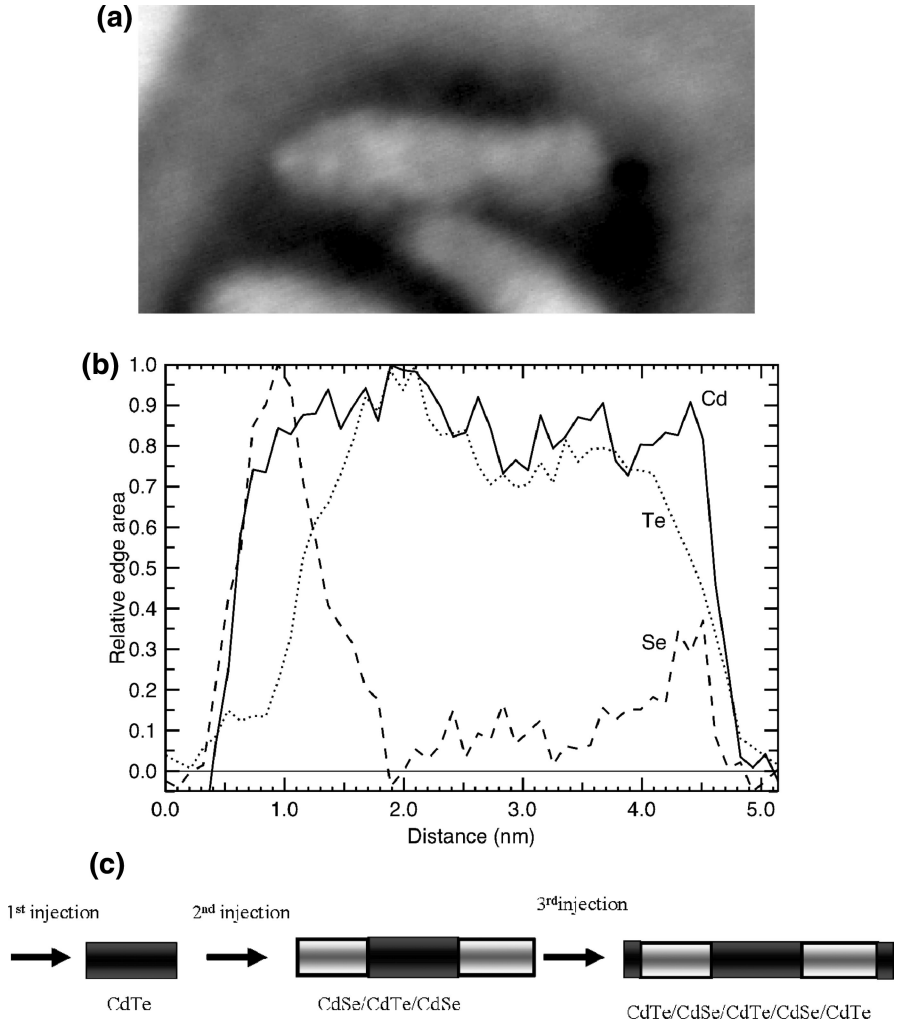


**Figure 5.** (a) HAADF image of the rod used for the EELS line scan. The line scan runs from left to right along the rod in the center of the image. (b) EELS line scan from the rod shown in (a). The values plotted are the measured areas of the Cd M45 edge at 404 eV (solid line), the Te $M_{4,5}$ edge at 572 eV (dotted line), and the Se $L_{2,3}$ edge at 1436 eV (dashed line) at each point, scaled to a maximum value of 1. Negative edge areas are due to noise in the background subtraction calculation. The image and line scans were taken using an accelerating voltage of 120 kV to reduce electron beam damage. (c) Diagram showing the growth sequence after each precursor injection.

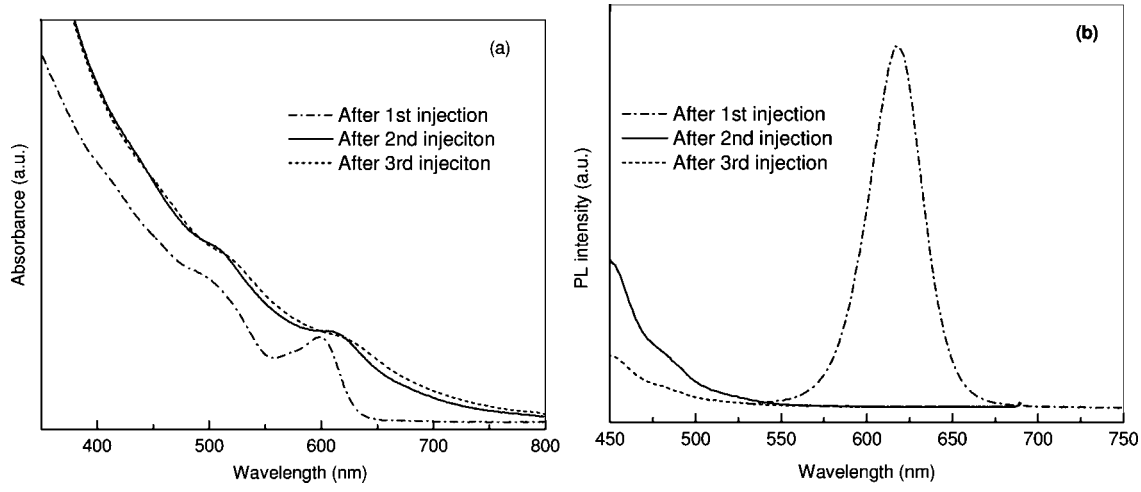


**Figure 6.** (a) UV−vis absorption and (b) PL spectra of as-prepared nanoparticles after the series of secondary precursors has been injected.

shape.[41] With the addition of the secondary precursor, the optical absorption of HNSs becomes weak and eventually disappears from the spectra, and the peak shifts slightly to longer wavelengths. If the length of the one-dimensional nanoparticles is bigger than the Bohr exciton diameter but the diameter of the nanoparticles is less than the Bohr exciton diameter, then the size-dependent shift in the optical spectra is solely related to the energy level quantization from the

nanoparticle's diameter.[33,42] Therefore, the shift in the spectra indicates that a thin shell has formed on the HNS rods (see also Figure 2b,c).[11] The lack of distinctive sub-band gap tails on the optical absorption spectra, which is observed from type-II core−shell quantum dots or core−shell tetrapods, is due to the same reason discussed above.[11,43] The absence of photoluminescence after the second injection (see Figure 6b) indicates that the secondary precursors significantly modify the electronic structure of the initial CdTe rods.[3,11] However, the real reason for the luminescence quenching in the HNSs is unclear at this moment. Milliron et al. and Peng et al. proposed that the high degree of charge separation occurring at the interfaces quenches the luminescence in the optical analysis.[3,11] Halpert et al. thought that since the carriers are spatially well separated, recombination occurs primarily through nonradiative pathways involving surface trap states.[25] This process makes the luminescence absent in the PL spectra of CdSe/CdTe nanobarbells. Saunders et al. proposed that quenching is a result of electron−hole recombination in both the CdSe block and across the CdSe|CdTe heterojunction after spatial separation.[28] Although several models are proposed for this system,[3,25,28,30] the complete understanding of the dynamics of exciton traps, charge separation, and recombination is still being studied. This is especially true for single heteronanostures.

## Conclusion

We have reported the growth of CdTe/CdSe multiblock HNSs using the hot coordinating solvents method. The formation of these structures is essential for future applications of semiconductor nanoparticles in nanoscale devices. In this study, it was found that the newly added precursor preferred to contribute to growth at the tips of previous formed nanocrystals. This is because in the presence of suitable ligands, the lateral nonpolar facets of wurtzite structure materials have much lower growth rates than the basal polar facets; therefore, the nanoparticles grew preferentially along their unique *c*-axis. HRTEM, HAADF, EELS line scans, and XRD were used to examine the chemical composition and the structure of these HNSs. This study may help the understanding of the growth of more complex functional nanomaterials.

CM802350P

(41) Shieh, F.; Saunders, A. E.; Korgel, B. A. *J. Phys. Chem. B.* **2005**, *109*, 8538.
(42) Steiner, D.; Katz, D.; Millo, O.; Aharoni, A.; Kan, S.; Mokari, T.; Banin, U. *Nano Lett.* **2004**, *4*, 1073.
(43) Kim, S.; Fisher, B.; Eisler, H. J.; Bawendi, M. *J. Am. Chem. Soc.* **2003**, *125*, 11466.